EUROPEAN ORGANIZATION FOR NUCLEAR RESEARCH

CERN-EP/81-17
9 March 1981

A MISSING-MASS SPECTROMETER FOR MOMENTA BELOW 1.5 GeV/c

G. D'Agostini[1], M. Arrignon[2], G. Auriemma[1], A. Bezaguet[4], J.P. de Brion[2], A. Caillet[2], J.B. Chèze[2], J. Derré[2], G. Ducastaing[2], G. Durand[2], E. Gennari[1], M. Lemoine[2], R. Llosa[5], G. Marel[2], G. Marini[1], G. Martellotti[1], F. Massa[1], A. Nigro[1], E. Pauli[2,4], C. Pigot[2], A. Rambaldi[1], S. Reucroft[3,4], C.E. Roos[3], B. Rothan[2], K. Schultze[4], A. Sciubba[1], S. Tentindo[1], G. Vrana[6], M. Webster[3,4] and E.G.H. Williams[3].

(Rome-Saclay-Vanderbilt Collaboration)

1) INFN and Ist. di Fisica, Rome University, Rome, Italy
2) DPHPE, CEN-Saclay, Gif-sur-Yvette, France
3) Dept. of Physics*, Vanderbilt University, Nashville, USA
4) CERN, Geneva, Switzerland
5) JEN, Madrid, Spain
6) Collège de France, Paris, France

ABSTRACT

An apparatus consisting of two magnetic spectrometers has been constructed at the CERN Proton Synchrotron (PS) in a missing-mass experiment to identify and select the beam particle and the outgoing one, and to measure their momenta. This paper gives details of the two spectrometers, which are comprised of multiwire proportional chambers, high resolution time-of-flight counters, and aerogel and water Čerenkov detectors.

(Submitted to Nuclear Instruments and Methods)

*) Research supported by NSF grant 73-08392.

1. INTRODUCTION

This paper describes the experimental apparatus installed at the CERN Proton Synchrotron (PS) for an experiment (PS 159) to search for narrow dibaryon states with strangeness -2 in the mass range $\sim$ 2.1 to 2.5 GeV/c^2, produced in the reaction

$$K^- + d \rightarrow K^+ + MM \qquad (1)$$

at an incident momentum of 1.4 GeV/c (where MM is missing mass). The outgoing K^+ is detected at very forward angles, i.e. in the low momentum transfer region.

To achieve the physics goals of this experiment, the following problems had to be solved:

i) A reasonable incident K^- flux implies a limited beam-line length, increasing the difficulty of obtaining a good separation between kaons and pions.

ii) In the forward direction, one has to distinguish the produced positive kaons from the high background of positive pions, due to the K^- decay into three pions, and of protons and pions produced at the target.

iii) The desired missing-mass resolution of a few MeV/c^2 required a measurement of the momentum of the incident particle with a resolution better than 0.2% at 1.4 GeV/c and of the outgoing one with $\Delta p/p^2 < 6.2 \times 10^{-3}$ $(GeV/c)^{-1}$. Particular care had therefore to be taken to minimize energy losses and multiple scattering.

iv) A considerable fraction of the outgoing K^+, whose mean momentum is $\sim$0.80 GeV/c, decay in flight in the first few metres.

All these problems were adequately solved and the apparatus was sufficiently versatile to allow the study of several other physical processes with only minor modifications (see section 10).

2. THE EXPERIMENTAL SET-UP

Protons from the CERN PS, of momentum 26 GeV/c, are made to impinge upon a tungsten target 50 mm long (see fig. 1). Approximately 60% of the protons interact, and the characteristics of the resulting charged secondary beam are[1]:

i) angular acceptance 2.2 msr; ii) maximum momentum 1.5 GeV/c; iii) momentum bite $\Delta p/p \approx \pm 2\%$; iv) length from the production target to the experimental focus 36.6 m. At the experimental target the beam components are 1.5×10^7 π^-, 1.9×10^7 π^+, 2.4×10^4 K^-, 3.3×10^4 K^+, 6×10^3 $\bar{p}$, and 3×10^6 p, for 1.6×10^{12} incident protons per machine pulse. The momentum is selected with the slit C_3, positioned after the bending magnet BM1, and the beam then passes through two 2 m and one 3 m electrostatic separators. The K^-/π^- ratio is a function of the mass slit C_4. When C_4 is opened to 1.2 mm, 80% of the K^- are kept and the ratio K^-/π^- is ~ 0.2.

The experimental set-up is shown in fig. 2. An aerogel Čerenkov counter $\check{C}_0$, of refractive index 1.05, is used to separate π from K and p at 1.4 GeV/c (see section 4), the separation being completed by means of the measurement of the time of flight (TOF) between the scintillators S_1 and S_2 (FWHM $\approx$ 250 ps, see section 3).

The beam spectrometer consists of four multiwire proportional chambers (MWPCs) (Ch_{11} before BM2; Ch_{12}, Ch_{13} and Ch_{14} after BM2), and measures the incident particle momentum with a resolution of 0.2% at 1.4 GeV/c.

A small scintillation counter P ($4 \times 3 \times 0.3$ cm^3), immediately in front of the target, is used for a better definition of the kaon beam, which is thus characterized by the coincidence $S_1 \cdot S_2 \cdot P \cdot \overline{\check{C}_0}$.

The liquid deuterium target is 40 cm long, with a diameter of 4 cm. It has four mylar windows in the beam with a thickness of 0.1 mm each, and it is surrounded by sixty 6 μm thick aluminized mylar foils.

The outgoing particle is detected in a forward magnetic spectrometer built around the dipole magnet VENUS (1.6 T·m, 1 m long, and of 1.65×0.4 m^2 aperture) whose centre is 278 cm from the centre of the target. The accepted range of momenta is $\sim$ 0.4–1.4 GeV/c, the central value being 0.80 GeV/c. The signature of the produced K^+ is partially obtained in the trigger logic by means of an aerogel Čerenkov counter $\check{C}_1$, of refractive index 1.094, which separates pions ($\gtrsim$ 0.32 GeV/c) from kaons ($\lesssim$ 1.12 GeV/c) and protons ($\lesssim$ 2.13 GeV/c), and with a water Čerenkov $\check{C}_2$ which

separates protons from kaons below about 1.1 GeV/c. The anticoincidence of the counter $\check{C}_1$ also eliminates the 1.4 GeV/c beam K^- which have not interacted in the target and whose decay in the spectrometer can generate spurious triggers. A high resolution TOF measurement (FWHM $\approx$ 350 ps, see section 3) between the counters S_2 and H_j, $\sim$ 5.5 m apart, allows the complete separation of different particles. The momentum of the particle is measured in the spectrometer through four large MWPCs (Ch_1 to Ch_4). A small chamber (Ch_{15}) is used to define more precisely the vertex of the interaction. A large scintillation counter, H_c, in front of the water Čerenkov counter $\check{C}_2$, is used to define the acceptance of the spectrometer.

The missing-mass resolution of the apparatus was tested in several reactions using a hydrogen target. In fig. 3 the mass of the Σ^+, as obtained in the reaction $\pi^+ p \to K^+\Sigma^+$ at 1.4 GeV/c is shown. The resolution is σ = 3.5 MeV/c^2, in agreement with expectation. The kinematics for reaction (1) is very similar, so that the expected resolution is approximately the same. The same reaction was used to test the over-all detection and analysis efficiency.

The acceptance for a dibaryon resonance was evaluated by a Monte Carlo program for different mass values, assuming an isotropic production in the centre of mass and taking in account the K^+ decay. The results are shown in fig. 4. It should be noted that if the resonance is produced preferentially at low momentum transfer, the value of the acceptance increases strongly.

Subsequent sections of this paper give more details on the characteristics of the TOF system, the aerogel and water Čerenkov's, the MWPCs, the electronics, the on-line and off-line programs, and the different trigger possibilities.

3. THE TIME-OF-FLIGHT MEASUREMENTS

The design of the TOF system is based upon a series of tests of different scintillators and light-guide configurations, as described in detail in another paper[2].

All the counters used for the TOF measurements are viewed by two Philips XP2020 photomultipliers (PMs) (photocathode diameter: 44 mm) at opposite sides; the two signals are recorded and then averaged.

The TOF of the beam particle is measured with the two PILOT U scintillation counters S_1 and S_2 (see fig. 2). Their geometry is shown in fig. 5. The distance between the two counters is $\sim$ 7.5 m and, for a momentum of 1.4 GeV/c, the TOFs are 25.1 ns for μ or π, 26.5 ns for K, and 30.1 ns for protons.

The TOF of the outgoing particle is measured between the scintillator S_2 and a hodoscope of nine PILOT U scintillators H_j ($25 \times 75 \times 2.5$ cm^3 each) placed at the end of the spectrometer (see figs. 2 and 5). The average path length of the measurement is $\sim$ 5.5 m. For a mean momentum of 0.80 GeV/c the TOF is 18.6 ns for μ and π, 21.5 ns for K, 28.3 ns for a proton, and 46.7 ns for a deuteron. It should be noted that we must be able to separate the produced particles up to $\sim$ 1.4 GeV/c, where these times become: 18.4 ns for μ and π, 19.4 ns for K, 22.1 ns for p, and 30.6 ns for d. A TOF resolution $\sigma \lesssim 0.2$ ns is therefore required.

While the incident particle can be identified only on the basis of the TOF measurements, a combined analysis of TOF, momentum, and path length is needed to identify the trigger particle, because it has a momentum spread of 400-1400 MeV/c and its path length in the spectrometer varies considerably.

Since the same counters are used for the trigger logic and for time measurements, the high-low technique is used to obtain, from each PM, a HIGH signal (output of a 300 mV threshold discriminator) for the logic and a LOW one (30 mV threshold) for the time analysis. For the mean value of the two LOW threshold crossing times of each counter, a pulse-height correction is computed by using the mean value $\langle A \rangle$ of the total charge collected at the anodes of the two PMs. The dependence of the time correction δt on $\langle A \rangle$ is assumed to have the form

$$\delta t = k \, (1/\sqrt{\langle A \rangle} - 1/\sqrt{A_0}) \ ,$$

where A_0 is arbitrarily chosen near the peak of the amplitude distribution. The actual value of k is obtained by analysing particles of known mass and momentum, and it turns out to be $k \simeq 5$ ns $\cdot$ pC$^{\frac{1}{2}}$ (see ref. 2).

In fig. 6 the beam TOF distribution is shown; the standard deviation is $\sigma = 0.11$ ns.

In fig. 7 the separation achieved for outgoing particles is shown. The mass M is reconstructed from the time of flight T between the counters S_2 and H_j, the momentum p, and the path length L, of the particle:

$$M^2 = p^2 \left[(T \times c/L)^2 - 1 \right] .$$

Actually, the TOF measured by each counter H_j contains an additive arbitrary constant T_{0j}. To obtain the correct value of T, we have calibrated the hodoscope with known particles, whose momentum and track length were measured by the MWPC system. Using the determined values of the constants T_{0j}, all the H_j counters can be gathered together, to give the over-all plot shown in fig. 7.

Figure 8 shows the time resolution obtained with one of the nine H_j counters. The standard deviation is $\sigma = 0.15$ ns. Under normal running conditions, when all nine spectra are superimposed, a standard deviation of about 0.2 ns is obtained, allowing a good separation of kaons and pions up to $\sim$ 1.4 GeV/c.

Under conditions of high intensity ($\gtrsim 10^6$ particles/s), accidental signals in the counters can give false starts or stops to the time-to-digital converters (TDCs). This effect is eliminated off line by requiring a correct correlation between HIGH and LOW threshold crossing times for the same PM, and between the LOW times of the two PMs of each counter (see ref. 2 for more details).

To ensure the long-term stability of the system, the PM gain and transit times are continuously checked during the data taking, by recording on line the time spectra and pulse-height distributions, and adjusting, if necessary, the high voltage.

4. THE AEROGEL ČERENKOV COUNTERS

The two aerogel Čerenkov counters $\check{C}_0$ and $\check{C}_1$ have been studied in a test beam and the results are reported elsewhere[3]. Their useful cross-sections are 10×8 cm^2 and 30×15 cm^2, respectively. Their geometry and physical characteristics

are shown in fig. 9. Each counter consists of a diffusing box partially filled with silica aerogel; each box is seen by two PMs.

The box of $\check{C}_0$ has a volume of $10 \times 8 \times 8$ cm^3. It is coated with two layers of millipore (a filter paper) and is viewed by two Philips XP2020 PMs (photocathode diameter: 44 mm). The box contains three aerogel blocks of refractive index 1.05; the radiator thickness along the beam is 7.5 cm.

The box of $\check{C}_1$ ($30 \times 15 \times 15$ cm^3) is also coated with millipore and is viewed by two Philips XP2041 PMs (photocathode diameter: 110 mm). The central region (R_1) of the box is filled with 12 aerogel blocks of refractive index 1.094, and around them there are 12 blocks of refractive index 1.06. This arrangement allows a lower threshold for particles crossing the central region of the counter. The radiator thickness along the beam is 9 cm.

Each PM is coupled to a cylindrical aluminized glass light-guide. The length of each light-guide is equal to the photocathode diameter and the transmission efficiency is $\sim$ 50%.

For incident pions of momentum 1.4 GeV/c, the average total number of photoelectrons collected by the two PMs of $\check{C}_0$ and $\check{C}_1$ was measured to be 17 and 22, respectively.

The spectrum of 1.4 GeV/c kaons in the counter $\check{C}_0$ corresponds to $\sim$ 0.06 photoelectrons.

The efficiency in the central region of $\check{C}_1$ was measured with π and K of different momentum. Figure 10 shows the mean number of collected photoelectrons as a function of the β of the incident particle. The residual scintillation below the threshold has also been measured and corresponds to $\sim$ 0.12 photoelectrons.

For both counters the two PMs are separately discriminated below the one-photoelectron level, and the OR of the two is sent to the logic.

5. THE WATER ČERENKOV COUNTER

The purpose of the water Čerenkov counter is to reject protons with momentum up to $\sim$ 1.1 GeV/c, copiously produced in the reactions $K^- + d \rightarrow p +$ anything. In this way the number of hardware triggers is reduced by a large amount.

Preliminary studies were performed on a test beam, and considerable improvement was achieved by adding to the water an amino G-salt wavelength shifter. A very large gain in the collected light was observed (about a factor of four) for a concentration of 10 mg per litre[4].

The counter is shown in fig. 11. It has a surface area of 227.5 × 75 cm^2 and a thickness of 16 cm. The inside surfaces of the aluminium box are coated with Nuclear Enterprise NE 560 titanium dioxide reflecting paint. The surface of the water is in contact with a 5 mm plexiglas window, which is optically connected to fourteen Philips XP2041 PMs (photocathode diameter: 110 mm). They are arranged along the top of the detector. The plexiglas light-guides are cylinders (13 cm diameter × 20 cm length) wrapped in aluminized mylar.

The gains of the fourteen tubes were equalized by scanning the counter with a pion beam. The fourteen outputs are resistively mixed, amplified by a factor of 10, and the resulting pulse fed into a discriminator. (Further details on the electronics are given in section 7.)

To select the suitable threshold, efficiency curves as a function of proton momentum, in the range 0.8–1.3 GeV/c, were measured for different values of the discriminator threshold. The results are shown in fig. 12. For the chosen threshold of 90 mV the efficiency rises from 10% to 90% for a change in momentum of less than 100 MeV/c. Analysis of the proton pulse-height distribution below threshold indicates that any scintillation contribution is negligible.

6. THE MULTIWIRE PROPORTIONAL CHAMBERS

The measurement of the spatial coordinates both of the beam and of the outgoing particle is realized by a system of nine MWPCs: Ch_{11}–Ch_{15} and Ch_1–Ch_4 of fig. 2. The total number of wires is 7300.

The characteristics of these chambers are summarized in Table 1. To reduce as much as possible multiple scattering, the cathodes of all chambers are made out of graphited mylar sheets, 50 μm thick. In the large chambers (Ch_1-Ch_4) the cathode mechanical rigidity is insufficient to avoid displacement under the electrical field used. Therefore the cathode-anode gap is kept constant by using spacers made of kapton garlands, 2 cm wide (see fig. 13a). Transverse, insulated, conducting wires, kept at high voltage, allow partial compensation of the electric field perturbation due to the presence of the garlands. The width of the dead region is about 2 cm.

The associated electronics is the one developed by a Saclay-Grenoble collaboration, whose basic circuit is the 8-channel PMOS integrated circuit "FILAS"[5]. A simplified diagram is shown in fig. 13b.

The chambers have been working for more than two years without major troubles. The average efficiency of each plane outside the spacer dead regions is about 96%.

The chamber Ch_{11} receives between 2×10^6 and 3×10^6 particle/s. With 100 ns WRITE gate, 20-25% of the events have a double hit in the chamber; such events are rejected by the off-line analysis.

7. THE ELECTRONICS

A simplified block diagram of the electronics logic used to study the reaction $K^- + d \rightarrow K^+ + MM$ is shown in fig. 14.

For the high-resolution TOF measurements, LeCroy circuits have been chosen, both for the fast logic (discriminators and coincidences) and for the analog-to-digital (ADC) and time-to-digital (TDC) converter units.

As can be seen in fig. 14, signals from all TOF photomultipliers are split into three. The first pulse ($\sim$ 10% of the input) is fed to a LeCroy 2249A ADC (1024 channels, 0.25 pC/channel). The second and the third signals are fed to LeCroy 621CL discriminators, one with a 30 mV threshold, the other with a 300 mV threshold, to give the LOW and the HIGH time pulses, respectively. The LOW pulse is then fed to a LeCroy 2228A TDC (1024 channels, 50 ps/channel) and used for the TOF measurement. The HIGH pulse is also fed to a TDC unit and used for rejection

of accidentals, as mentioned in section 3. The OR of the HIGH pulses from the two PMs of the same counter is used for the trigger logic. Furthermore, to reduce pile-up at the input of the TDC, the LOW signals are gated by the logic OR of the corresponding HIGH pulses.

The scheme of the trigger logic is straightforward. The S_1 counter, in coincidence with $(S_2 \cdot P)$, provides the "beam" signal. The anticoincidence of $\check{C}_0$ identifies the K of the beam ("K^- beam" signal). Since only one particle is required to pass through the spectrometer, the OR outputs of the nine hodoscope counters H_j are sent to a multiplicity unit. The output "$m_H = 1$", corresponding to only one H_j counter fired, is set in coincidence with the "K^- beam", the H_c counter (which defines geometrically the acceptance of the spectrometer), and the Čerenkov $\check{C}_2$ (which rejects protons $\lesssim 1.1$ GeV/c), to give the "interaction" signal. Finally, the anticoincidence of the Čerenkov $\check{C}_1$ selects the "master" events, electronically defined for reaction (1) as

$$(S_1 \cdot S_2 \cdot P \cdot \overline{\check{C}_0}) \cdot (m_H = 1) \cdot (H_c \cdot \check{C}_2) \cdot \overline{\check{C}_1} \ .$$

The "master" signal is sent to the CAMAC fast gate (Saclay Porte Rapide) which initializes the read-out cycle and triggers the WRITE signals sent to all the chamber planes. The start to the TDC circuits (as well as the gate to the ADCs) is provided by special masters, MS_{1A} and MS_{2A}, which are in time with the S_{1A} and S_{2A} PM signals, respectively. In this way, it is possible to perform an accidental-rejection procedure which is described in detail in ref. 2. Such a procedure eliminates the majority of the accidental events, whose number would not be negligible under high flux running conditions ($\gtrsim 10^6$ particles/s).

The total delay time between the physical occurrence of the event and the arrival of the master signal at the input of the CAMAC fast gate, is about 300 ns. It results from about 30 ns PM delay, 75 ns cables from the apparatus to the counting room, and about 200 ns due to the electronics and the timing requirements.

Twenty thousand K^- per machine pulse produce, on a deuterium target, about 120 "interaction" events. With $\check{C}_1$ in anticoincidence the number of master triggers

per burst becomes about 16. An on-line analysis on the NORD-10S computer (see section 8) reduces the number of events collected on tape to a rate of about 0.8 per burst).

Finally, we note that as well as reaction (1), we have also investigated several other physical processes which are listed in section 10. For some of these reactions minor changes have to be performed in the logic. For example, the Čerenkovs $\check{C}_0$, $\check{C}_1$, and $\check{C}_2$ can be independently included or removed from the master. In addition, signals from a system of counters surrounding the target can be included in the trigger, in order to reduce the high counting rate associated with some of the considered reactions (see again section 10).

8. THE ON-LINE PROGRAM

The on-line program has been written for performing three different tasks: i) data acquisition; ii) test of the set-up; iii) data reduction. The latter task had to be achieved with a rather flexible program, according to the particular needs of the different reactions studied. With this aim it was decided to write it in real-time FORTRAN.

The hardware configuration is as follows. The computer is a Norsk-Data NORD-10S with 96K resident memory and 1K cache memory, coupled to a double disk of 10 Mbytes, a 1600 bpi 75 ips magnetic tape unit, two alphanumeric terminals and one Tektronix 4006 graphic terminal. The resident operating system is a disk time-sharing one, and the computer is coupled to CAMAC through a GEC Eliott interface.

The software configuration was obtained by implementing the standard CERN Data Acquisition Program DAS[6], adapted to the peculiar needs of our experiment. The memory space occupied by the different tasks within DAS is as follows: ZDAS 20K; ZPHYS 18K; ZMONX 4K. The time needed for the data acquisition is $\sim$ 3 ms per event.

The possibility of testing the correct performance of the different detectors of the experiment is obtained by histogramming a large number of data such as TOFs,

counter pulse-heights, wire chamber efficiencies, etc. Crucial quantities, such as magnet currents, for example, are directly tested by the computer through digital voltmeters. Furthermore, a fast approximate analysis allows one to calculate and display several physical quantities such as the momentum of the beam or of the outgoing particles, the vertex of the interaction, and even the missing mass for a pre-specified reaction.

The aim of the on-line data-reduction program was to reject as many bad triggers as possible in order to reduce the amount of data to be analysed off-line. This task is executed between PS spills and the program is compact enough to avoid swapping between disk and central memory. The on-line program is able to process up to $\sim$ 80 events per burst, which have been previously stored in a 31 Kword temporary buffer (340 words per event) during the spill. After this procedure the number of accepted events may be reduced to a few per cent of the initial triggers.

To be "accepted" an event must fulfil the following selection criteria:

i) Meaningful response from all the TDCs.

ii) Good efficiency in the wire chambers, i.e. it must have enough hits for reconstructing the particle momentum.

iii) Outgoing particle mass and momentum in the desired range. This information is obtained by a point-finding procedure in the chambers followed by a rough track reconstruction. This method is accurate enough to select only the physical track and to measure its momentum and length. The TOF measurement completes the information needed to reconstruct the mass M of the particle (see fig. 15).

In some cases we have also required:

iv) Only one beam particle.

v) Correct TOF for the beam particle.

All these conditions can be totally or partially relaxed or modified to allow data taking for different reactions or for test runs, etc.

9. THE OFF-LINE PROGRAM

The off-line analysis is based on the program PRATIC, derived from the program PATRAC[7]. Written in FORTRAN for the CDC 7600, it uses the dynamic memory optimization program ZBOOK[8] and the histogramming facility HBOOK[9].

The program is structured in four levels:

i) INPUT SECTION: to decode either the information from the primary data tapes or from data summary tapes created in a preceding step.

ii) ANALYSIS SECTION: to calculate the relevant physical parameters of the beam and the outgoing particle. This section can be subdivided into several stages: a) computation of the momentum and the TOF for the incident particle; b) point-finding in the four large chambers of the VENUS spectrometer; c) track-finding, through the method of principal components, to obtain the physical outgoing track; d) rejection of particles decaying along the spectrometer by a constrained fit performed on the outgoing track; e) reconstruction of the vertex of the interaction; f) reconstruction of the mass of the outgoing particle through the TOF information.

iii) KINEMATICS SECTION: to compute the kinematics of the event, taking into account appropriate corrections, such as energy losses, to the measured parameters.

iv) TOF SECTION: a quite independent section to allow the determination of the calibration constants used for the identification of the incident and of the outgoing particle through the TOF measurements.

The efficiency of the analysis procedure has been tested by studying subsamples of the data. It depends weakly upon the considered physical reaction and is estimated to be $\sim$ 85%, mainly because of inefficiencies of the wire chambers and the presence of more than one hit in chamber 11.

10. OTHER EXPERIMENTAL POSSIBILITIES

As mentioned in the Introduction, the apparatus was designed to allow the study of other processes as well as reaction (1). In practice this has been achieved mainly by changing the role in the trigger of the Čerenkov counters $\check{C}_0$ and $\check{C}_1$.

We have collected data, at various beam energies, in the following reactions:

$$K^- d \to \pi^\pm + MM \ , \qquad \text{trigger: } \overline{\check{C}_0}\ \check{C}_1 \tag{2}$$

$$\pi^\pm d \to K^+ + MM \ , \qquad \text{trigger: } \check{C}_0\ \overline{\check{C}_1} \tag{3}$$

$$\bar{p}p \to \pi^+ + MM \ , \qquad \text{trigger: } \overline{\check{C}_0} \ . \tag{4}$$

Of course, the selection criteria of the on-line data reduction program were changed accordingly to reject the bulk of the undesired triggers.

In addition, our set-up was implemented with a system of scintillation counters surrounding the target almost completely (see fig. 16). For some of the above-mentioned reactions it was necessary to ask in the trigger for hits in at least one (or, sometimes, at least two) of these counters, in order to reduce the high trigger rate due to the non-interacting beam passing through the spectrometer (this is the case when the requested outgoing particle has the same sign as the incident beam). In these circumstances, the detection efficiency of the apparatus is reduced, depending on the specific process, by a factor which had to be evaluated using a Monte Carlo simulation program. However, these losses in statistics are compensated for by a gain in the available information on the products of the reaction: in some cases, a multiplicity analysis has substantially increased the signal to the physical background ratio.

Acknowledgements

We are greatly indebted to CERN for its hospitality. We wish especially to thank all the CERN technical staff for invaluable support.

REFERENCES

1) See section on beam k_{24} *in* M. Ferro-Luzzi and G. Petrucci, Secondary beams for tests and counter experiments at the CPS for the year 1979, Internal Report CERN-EP/79-05 (1979).

2) G. D'Agostini, G. Marini, G. Martellotti, F. Massa and A. Sciubba, High resolution time-of-flight measurements in small and large scintillation counters, Preprint CERN-EP/80-228 (1980), to be published in Nucl. Instrum. Methods.

3) J.P. de Brion, A. Caillet, J.B. Chèze, J. Derré, G. Marel, E. Pauli, C. Pigot and G. Vrana, Nucl. Instrum. Methods 179, 61 (1981).

4) A. Bezaguet, C. Geles, S. Reucroft, G. Marini and G. Martellotti, Nucl. Instrum. Methods 158, 303 (1979).

5) P. Bareyre, P. Borgeaud, J. Poinsignon and B. Billion, Nucl. Instrum. Methods 131, 583 (1975).
J. Poinsignon, Nucl. Instrum. Methods 156, 141 (1978).

6) A. Bogaerts, DAS, the Nord-10 data acquisition system, CERN NORD Program Library 780406 (1978).

7) R. Brun, PATRAC NA4 analysis program, version 2, CERN DD/EE/79-3 (1979).

8) R. Brun, M. Hansroul and J.C. Lassalle, ZBOOK user guide and reference manual, CERN DD/77-10 (1977).

9) R. Brun, I. Ivanchenko and P. Palazzi, HBOOK user guide, version 3, CERN DD/77-09 (1978).

Table 1

Characteristics of the MWPCs. X is the horizontal coordinate, Y the vertical one, and U is inclined by 14° with respect to the X axis.

Chamber number	No. of planes	Sensitive region dimensions (mm)			Gap	Wire spacing	Wire diameter
		ΔX	ΔY	ΔU	(mm)	(mm)	(μm)
1	3	448	480	416	8	2	20
2	3	704	640	672	8	2	20
3	3	1744	512	1888	8	2	20
4	3	2016	512	2016	8	2	20
11	2	64	128	-	5	1	10
12	2	128	128	-	5	1	10
13	2	128	96	-	5	1	10
14	2	128	128	-	5	1	10
15	2	192	192	-	5	1	10

Figure captions

Fig. 1 : The k_{24} beam line.

Fig. 2 : The experimental set-up.

Fig. 3 : Missing-mass distribution for the reaction $\pi^+ p \to K^+ + MM$.

Fig. 4 : Acceptance ε of the experimental apparatus for a dibaryon state, assuming an isotropic production in the centre of mass: solid line. The dashed line shows the acceptance obtainable without requiring the Čerenkov $\check{C}_2$ in the trigger.

Fig. 5 : The TOF counters: a) S_1 and S_2; b) H_j.

Fig. 6 : Beam TOF distribution.

Fig. 7 : Reconstructed momentum p of the outgoing particle versus calculated mass squared M^2.

Fig. 8 : Typical TOF resolution from one of the H_j counters. The distance between S_2 and H_j is $\sim$ 5.5 m. — Uncorrected TOF (σ = 0.28 ns, $\Delta T_{5\%}$ = = 1.25 ns); --- PH-corrected TOF (σ = 0.15 ns, $\Delta T_{5\%}$ = 0.65 ns).

Fig. 9 : The Čerenkov counters $\check{C}_0$ and $\check{C}_1$.

Fig. 10 : Mean total number of photoelectrons n_{ph} versus β for Čerenkov $\check{C}_1$, measured with π and K of different momentum.

Fig. 11 : The water Čerenkov counter $\check{C}_2$ (dimensions are in mm).

Fig. 12 : Efficiency curve of $\check{C}_2$ for different values of the discriminator threshold, as a function of proton momentum.

Fig. 13 : a) Schematic structure of the garlands.
b) Simplified diagram of a MINIFILAS. Each JCF10 circuit is for one chamber plane read-out.

Fig. 14 : Diagram of the electronics logic.

Fig. 15 : Calculated mass squared M^2 of the outgoing particle from the on-line analysis.

Fig. 16 : T-counter set-up.

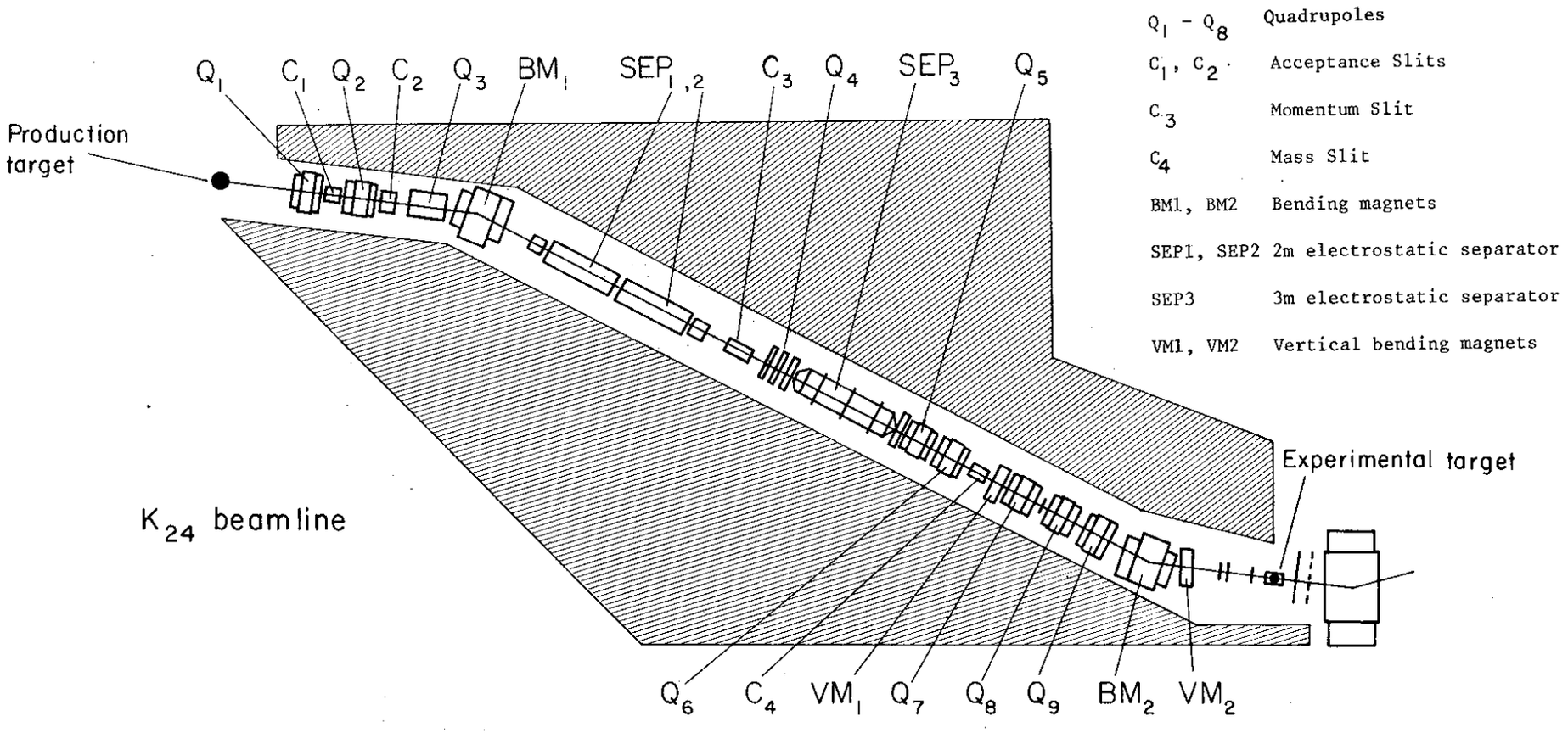
Q1
C1
Q2
C2
Q3
BM1
SEP1,2
C3
Q4
SEP3
Q5
Production target
K24 beamline
Experimental target
Q6
C4
VM1
Q7
Q8
Q9
BM2
VM2
Q1 - Q8 Quadrupoles
C1, C2 Acceptance Slits
C3 Momentum Slit
C4 Mass Slit
BM1, BM2 Bending magnets
SEP1, SEP2 2m electrostatic separator
SEP3 3m electrostatic separator
VM1, VM2 Vertical bending magnets

Fig. 1

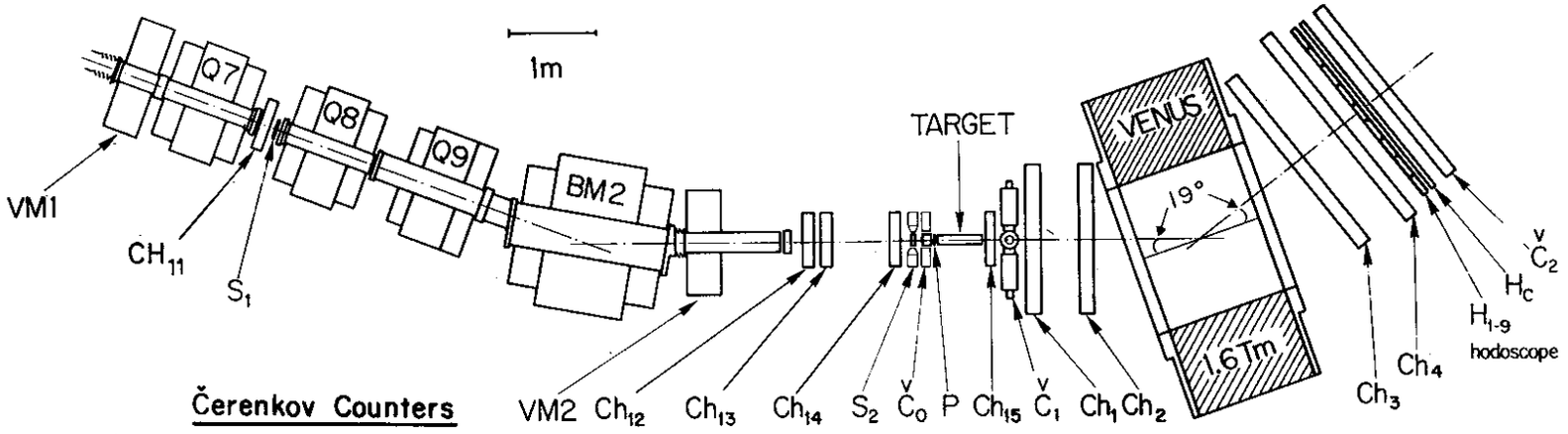

Čerenkov Counters

$\breve{C}_0$: Aerogel (n=1.05)

$\breve{C}_1$: Aerogel (n=1.094)

$\breve{C}_2$: Water with wave-length shifter

Multi Wire-Proportional-Chambers

$Ch_{11,12,13,14,15}$: 1mm spacing MWPC

$Ch_{1,2,3,4}$: 2mm spacing MWPC

Scintillation Counters

S_1 :	PILOT-U Scintillator	5x10x0.5 cm³
S_2 :	PILOT-U Scintillator	5x10x 1 cm³
P :	NE 110 Scintillator	4x 3 x 0.3cm³
H_j (j=1,,9):	PILOT-U Scint.	25x75x2.5cm³
H_c :	NE 110 Scintillator	225x55x 1 cm³

Fig. 2

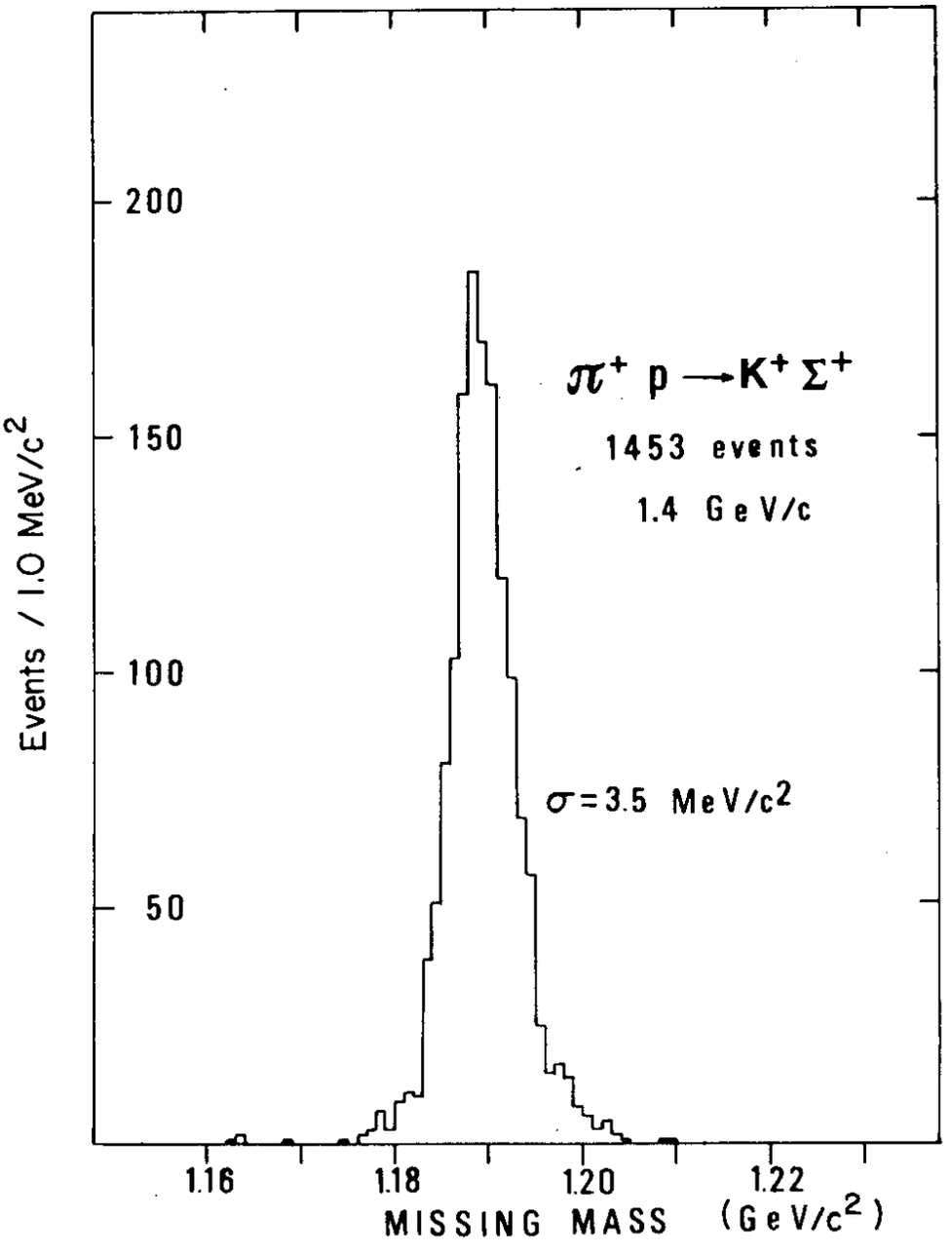
200
150
100
50
Events / 1.0 MeV/c²
π⁺ p → K⁺ Σ⁺
1453 events
1.4 GeV/c
σ = 3.5 MeV/c²
1.16
1.18
1.20
1.22
MISSING MASS (GeV/c²)

Fig. 3

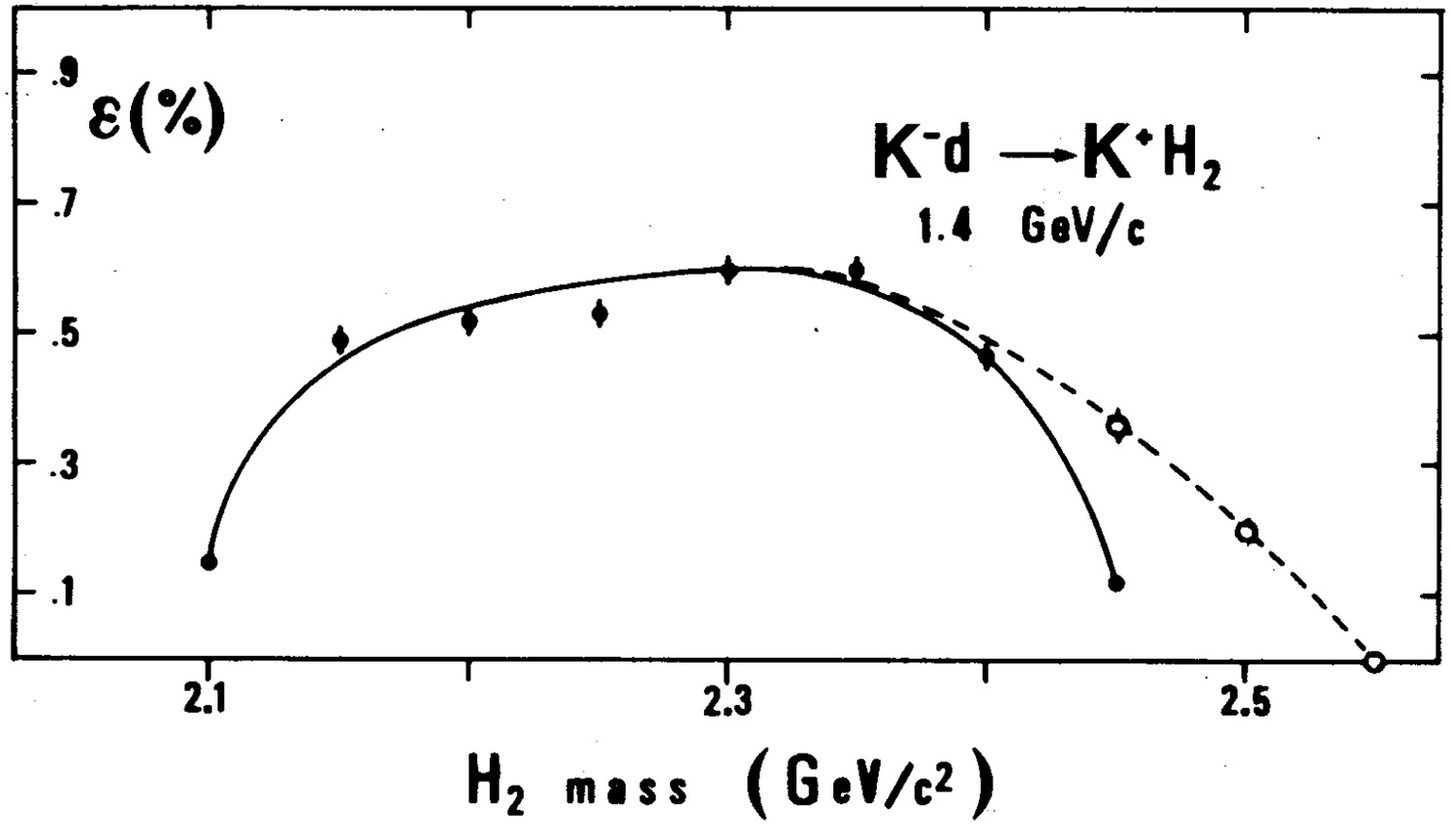

Fig. 4

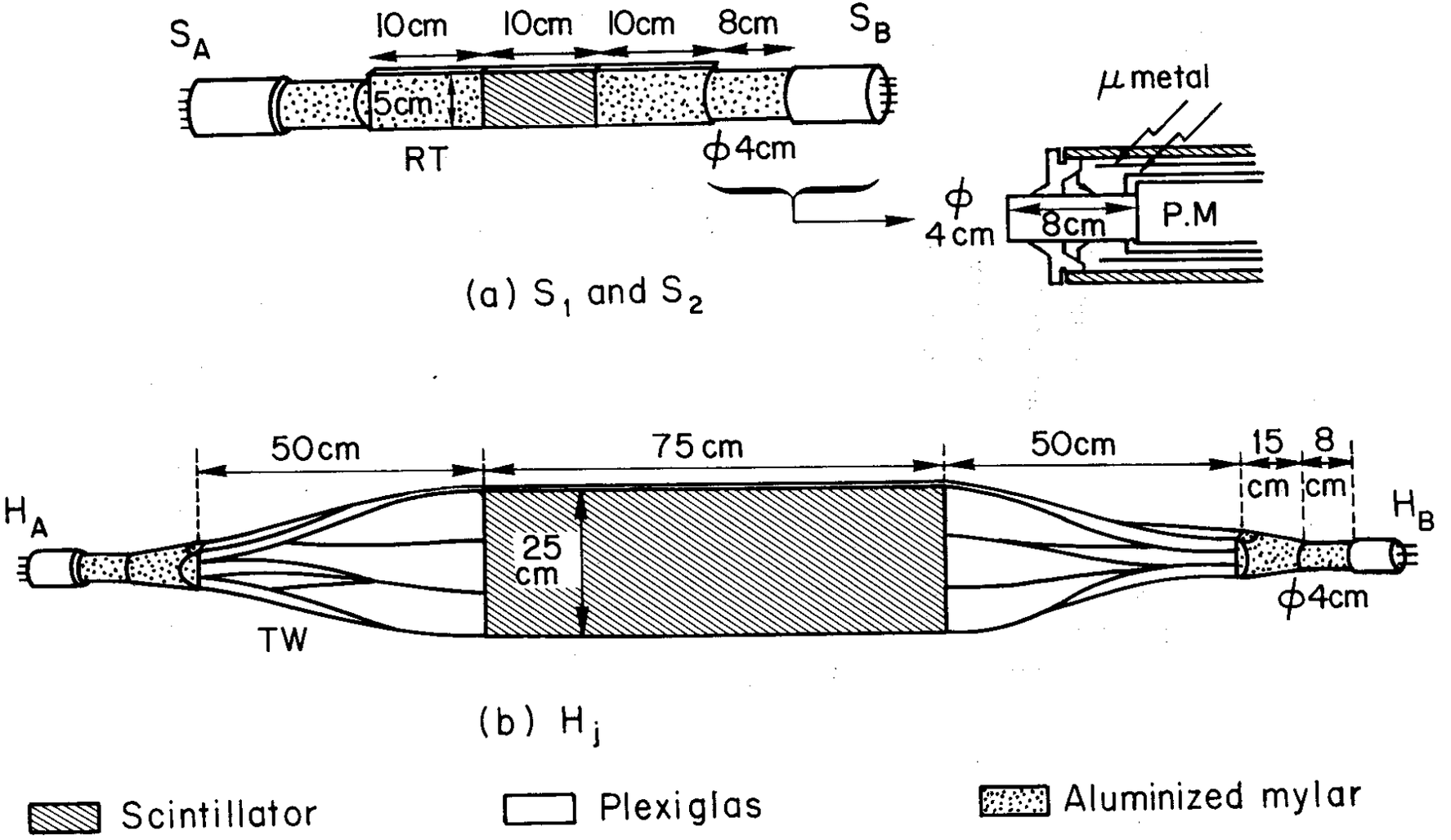
S_A
10cm
10cm
10cm
8cm
S_B
5cm
RT
φ4cm
μ metal
φ
4 cm
8cm
P.M
(a) S_1 and S_2
50cm
75 cm
50cm
15
cm
8
cm
H_A
H_B
25
cm
TW
φ4cm
(b) H_j
Scintillator
Plexiglas
Aluminized mylar

Fig. 5

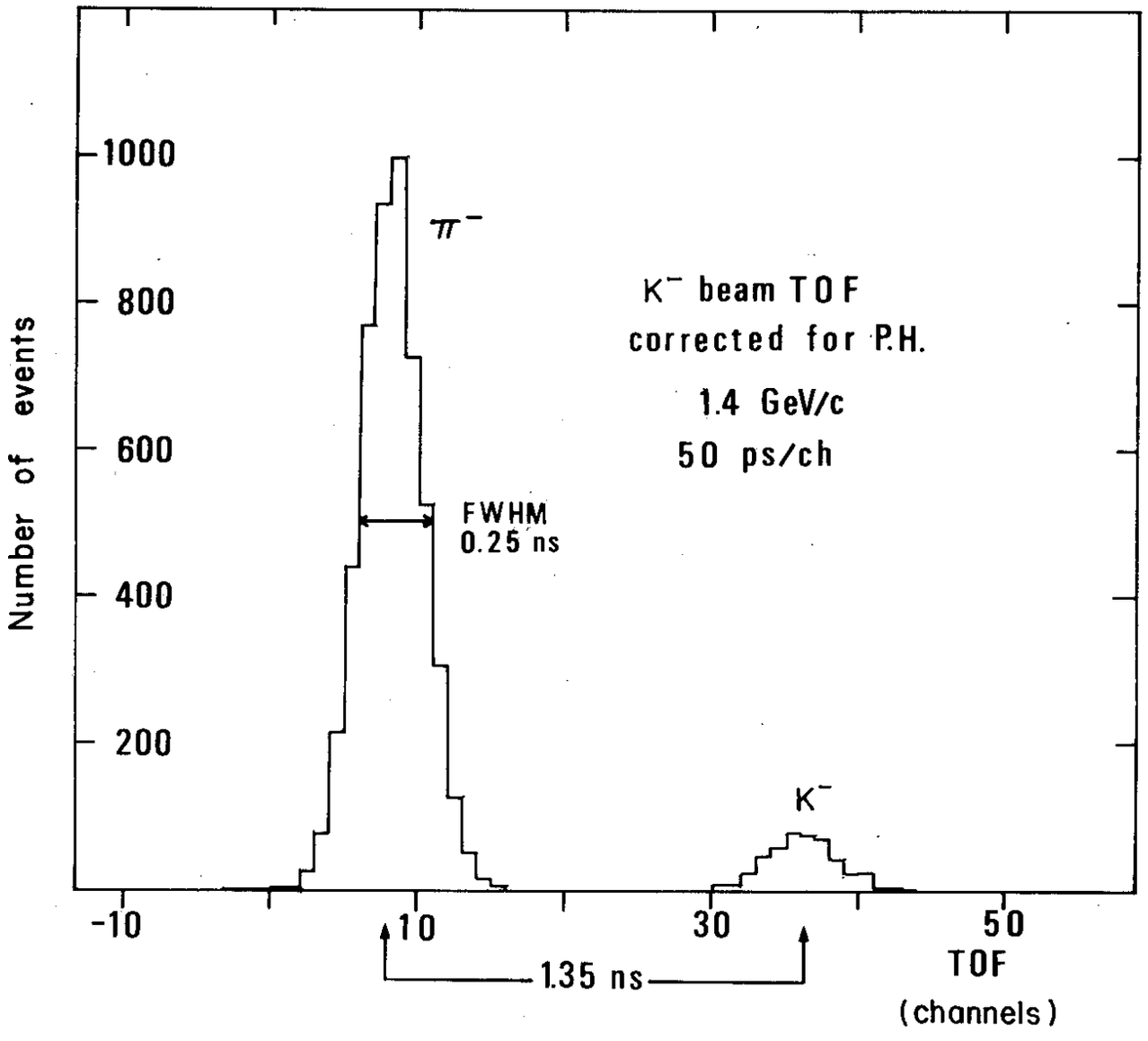
Number of events
1000
800
600
400
200
π^-
K^- beam TOF
corrected for P.H.
1.4 GeV/c
50 ps/ch
FWHM
0.25 ns
K^-
-10
10
30
50
1.35 ns
TOF
(channels)

Fig. 6

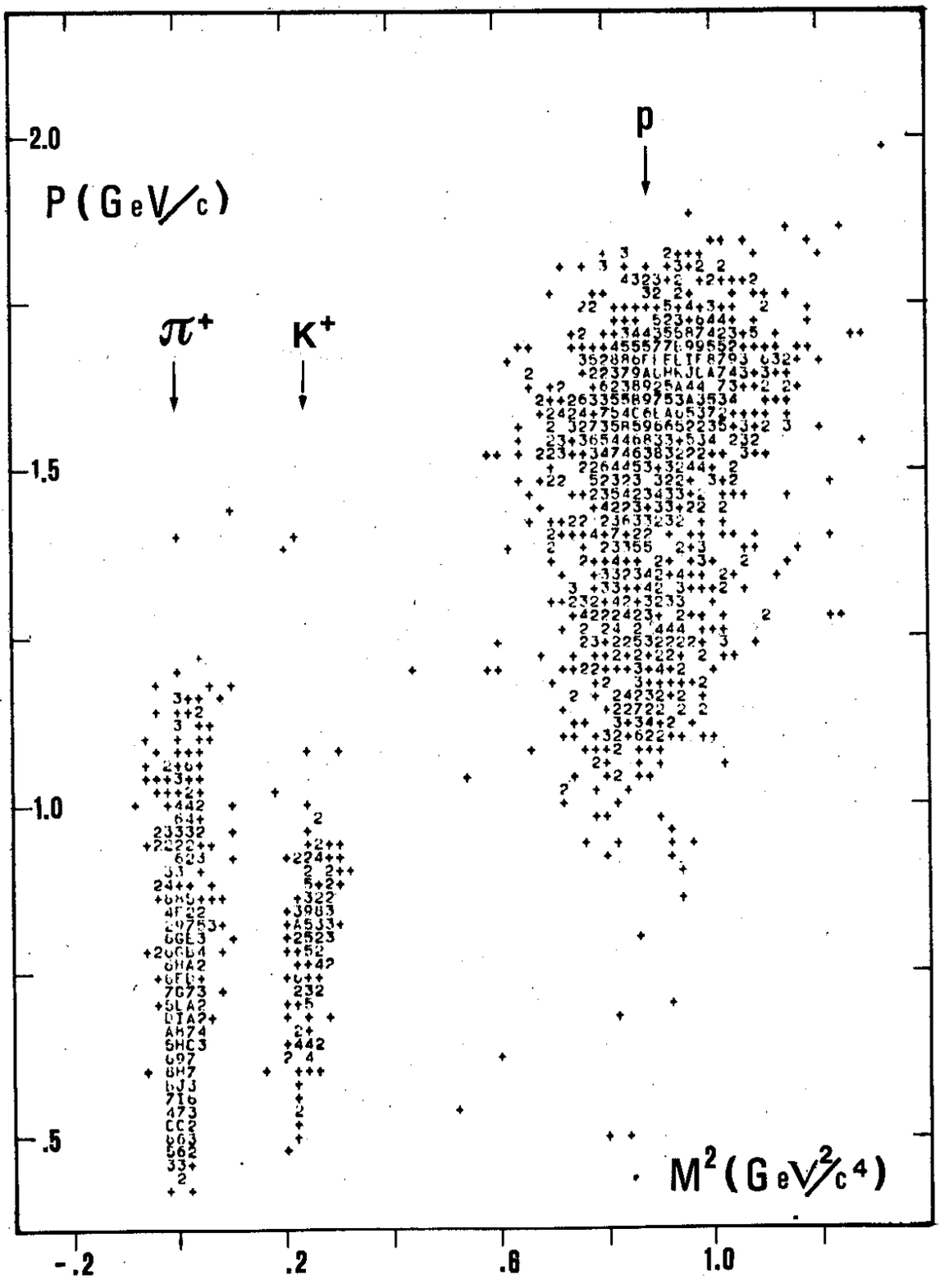

Fig. 7

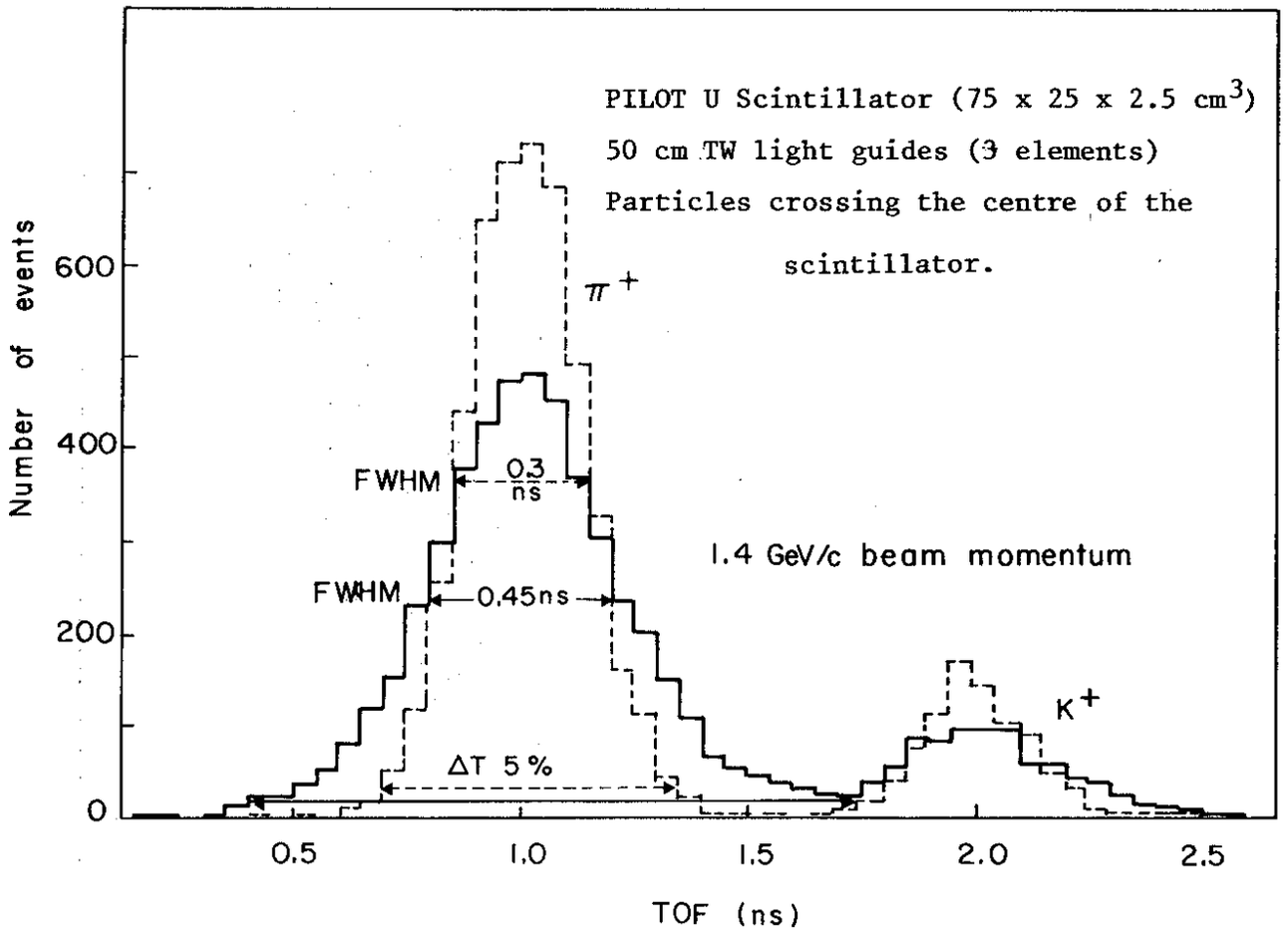
PILOT U Scintillator (75 x 25 x 2.5 cm^3)
50 cm TW light guides (3 elements)
Particles crossing the centre of the scintillator.
1.4 GeV/c beam momentum
π^+
K^+
FWHM
0.3 ns
FWHM
0.45ns
ΔT 5 %
Number of events
TOF (ns)
0
200
400
600
0.5
1.0
1.5
2.0
2.5

Fig. 8

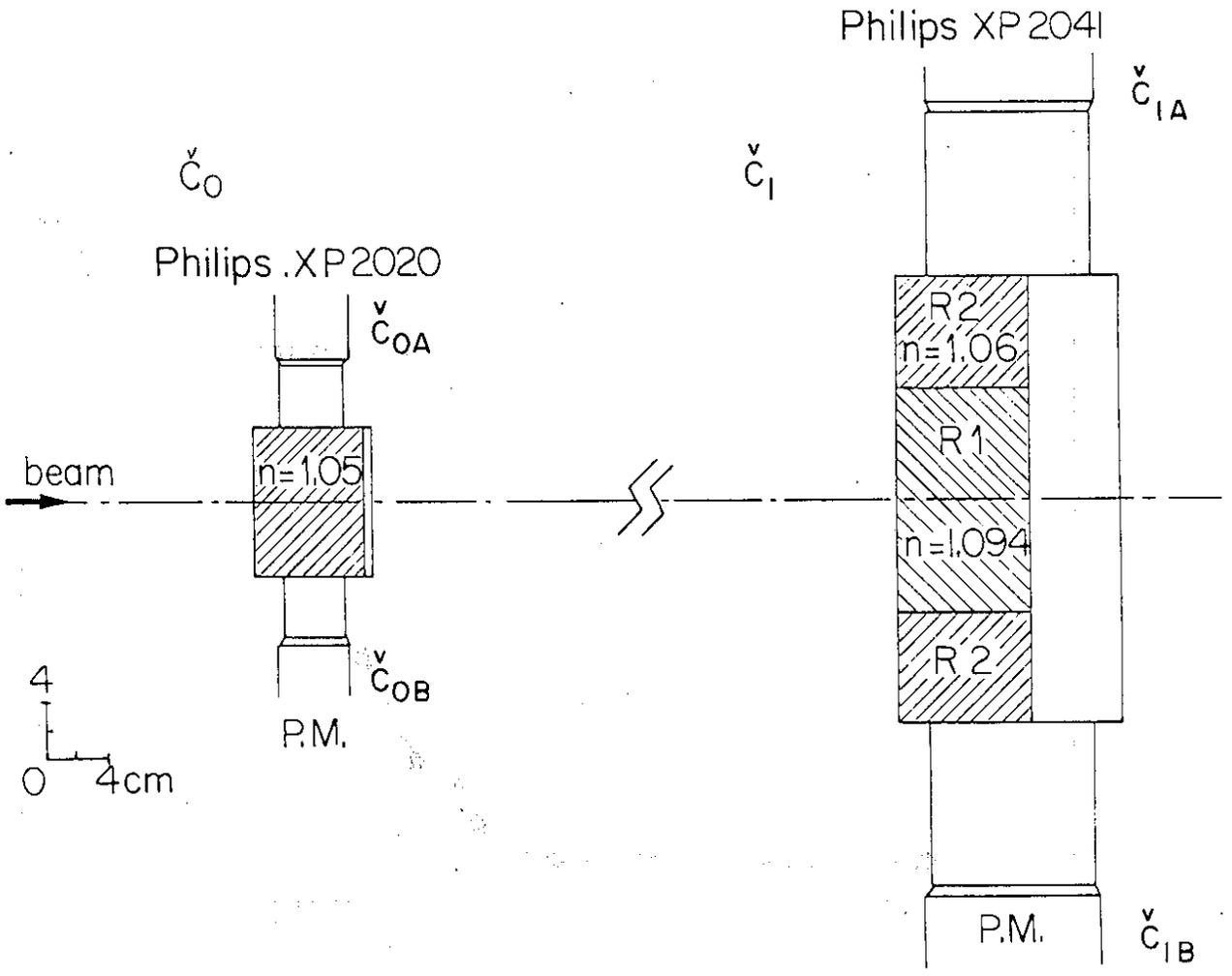
Philips XP2041
$\check{C}_{1A}$
$\check{C}_0$
$\check{C}_1$
Philips .XP2020
$\check{C}_{0A}$
R2
n=1.06
R1
beam
n=1.05
n=1.094
R2
$\check{C}_{0B}$
4
0
4cm
P.M.
P.M.
$\check{C}_{1B}$

Fig. 9

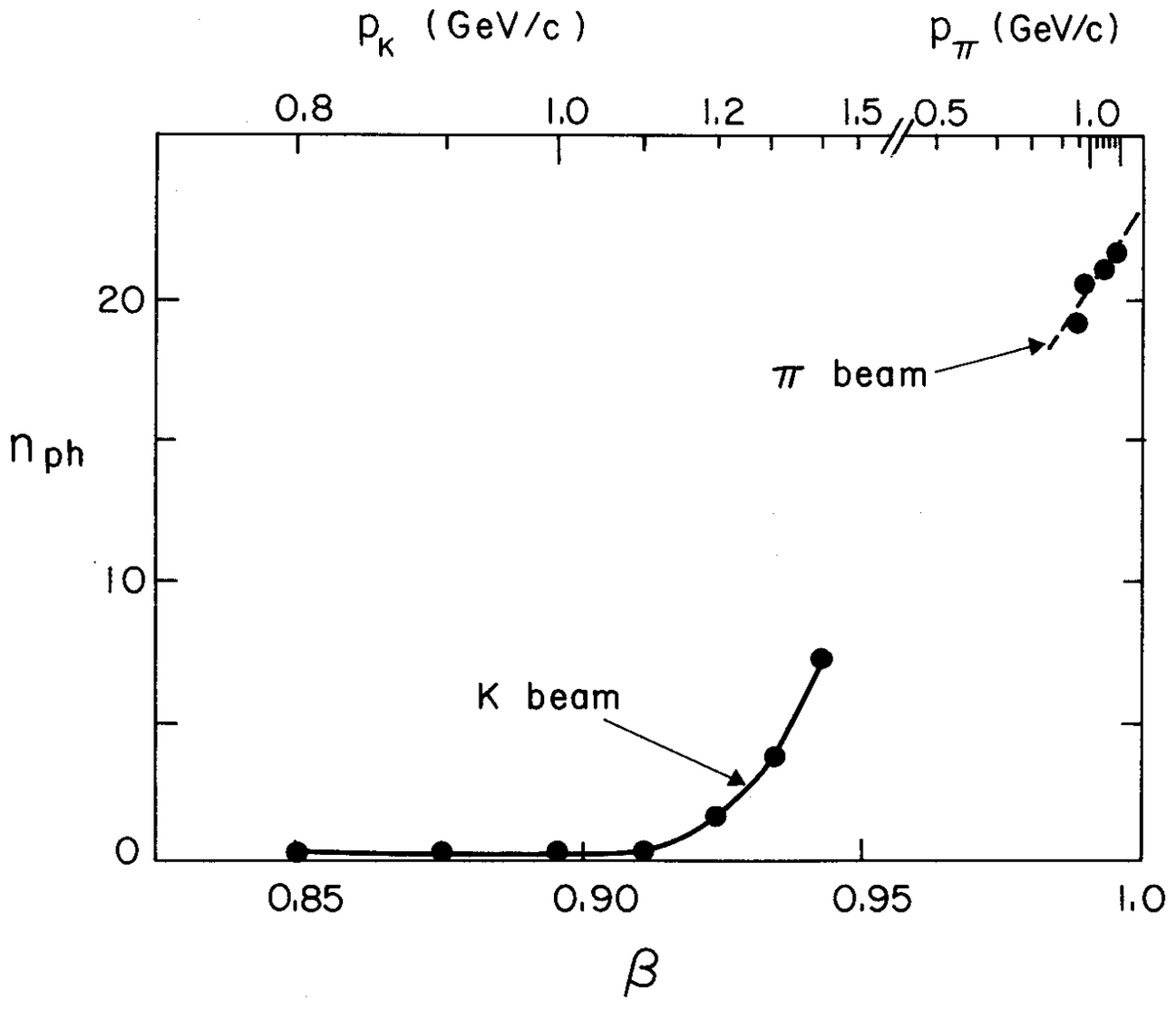
p_K (GeV/c)
p_π (GeV/c)
0.8
1.0
1.2
1.5
0.5
1.0
20
10
0
n_{ph}
π beam
K beam
0.85
0.90
0.95
1.0
β

Fig. 10

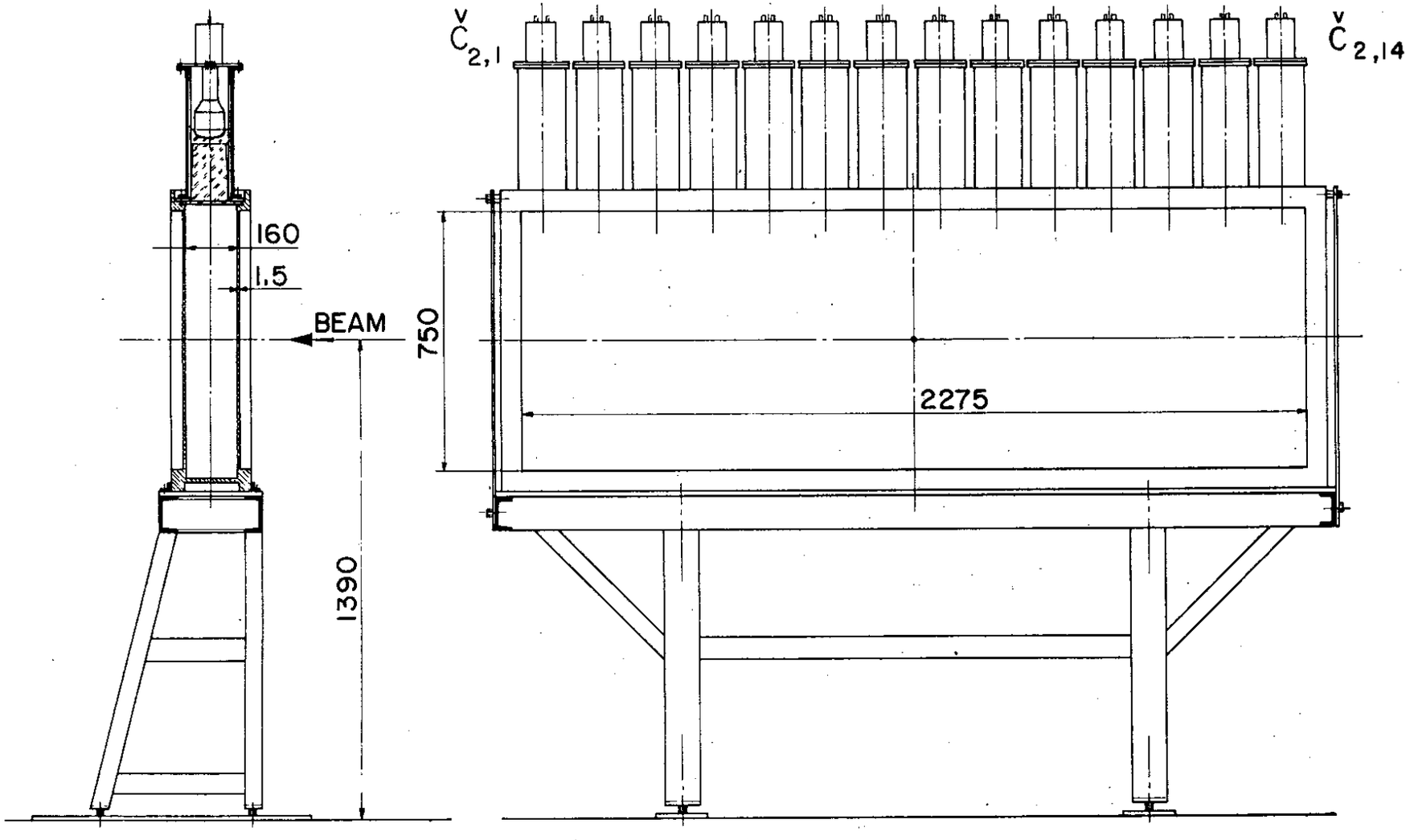

Fig. 11

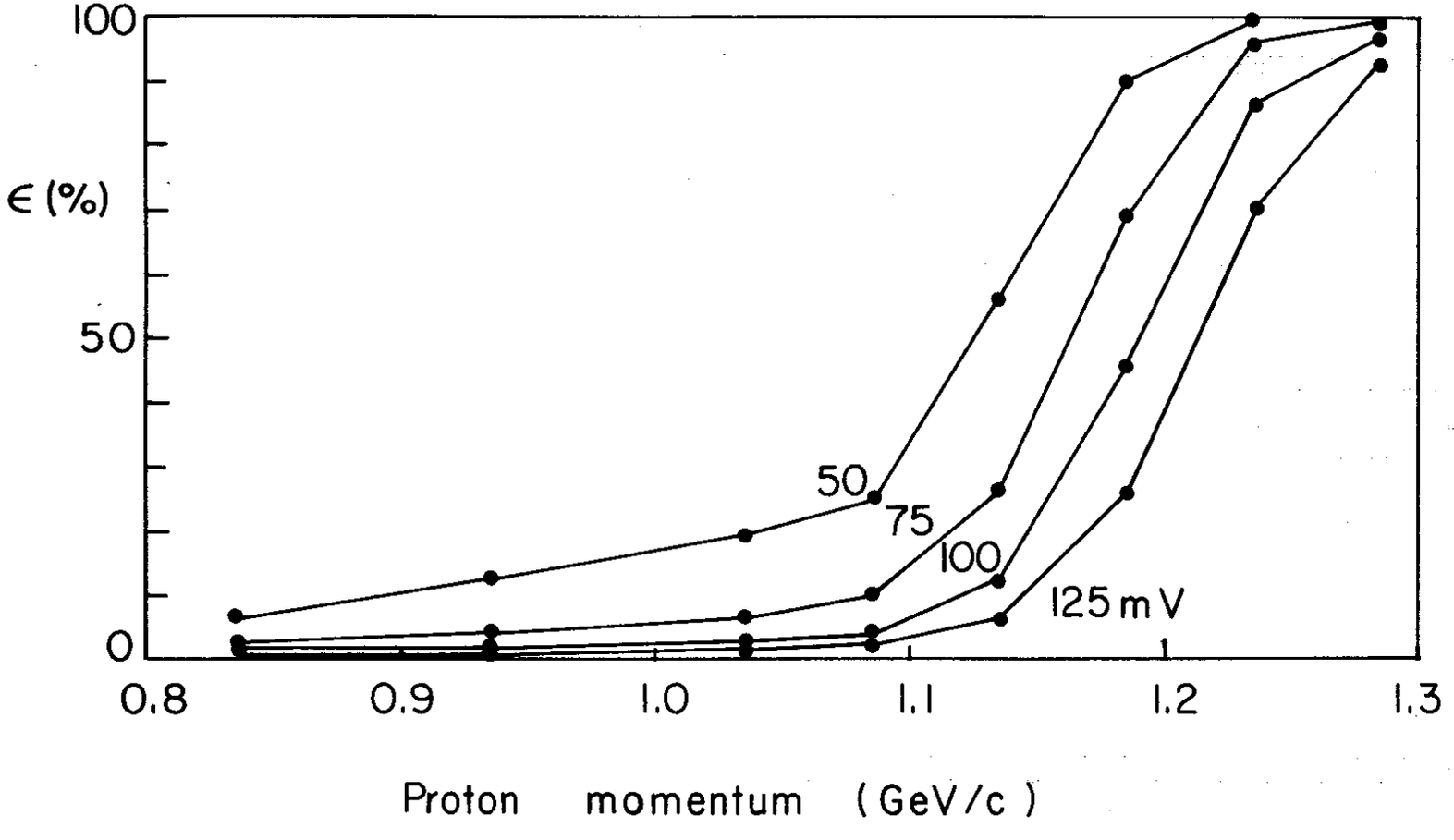

Fig. 12

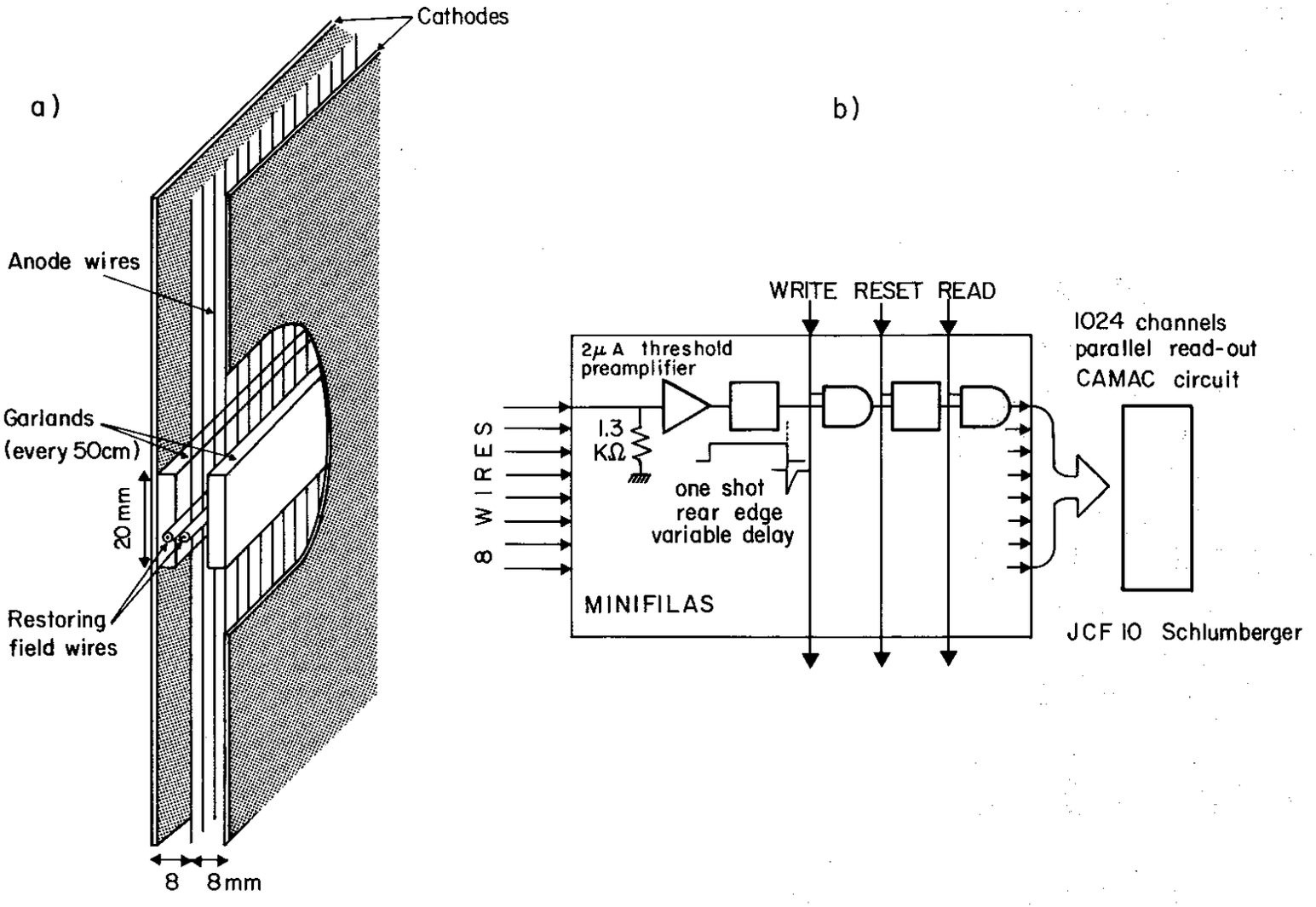
a)
Cathodes
Anode wires
Garlands
(every 50cm)
20 mm
Restoring
field wires
8
8mm
b)
WRITE RESET READ
2μA threshold
preamplifier
1.3
KΩ
one shot
rear edge
variable delay
8 WIRES
MINIFILAS
1024 channels
parallel read-out
CAMAC circuit
JCF 10 Schlumberger

Fig. 13

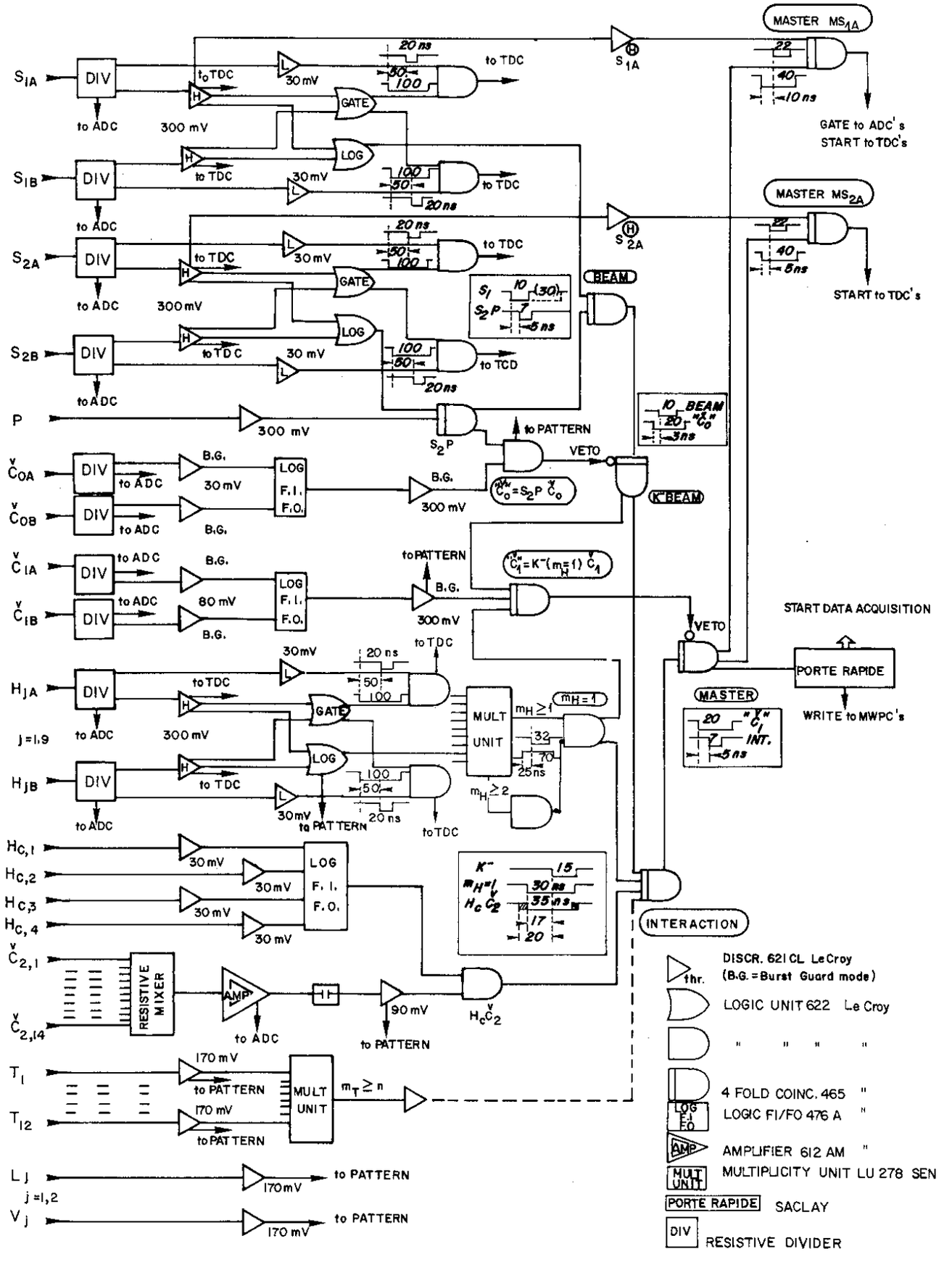
MASTER MS1A
MASTER MS2A
GATE to ADC's
START to TDC's
START to TDC's
START DATA ACQUISITION
PORTE RAPIDE
WRITE to MWPC's
BEAM
K⁻BEAM
VETO
INTERACTION
MASTER
DIV
LOG
GATE
MULT UNIT
RESISTIVE MIXER
AMP
LOG F.I. F.O.
to ADC
to TDC
to PATTERN
300 mV
30 mV
80 mV
170 mV
90 mV
B.G.
DISCR. 621 CL LeCroy
(B.G. = Burst Guard mode)
LOGIC UNIT 622 Le Croy
4 FOLD COINC. 465 "
LOGIC FI/FO 476 A "
AMPLIFIER 612 AM "
MULTIPLICITY UNIT LU 278 SEN
PORTE RAPIDE SACLAY
RESISTIVE DIVIDER

Fig. 14

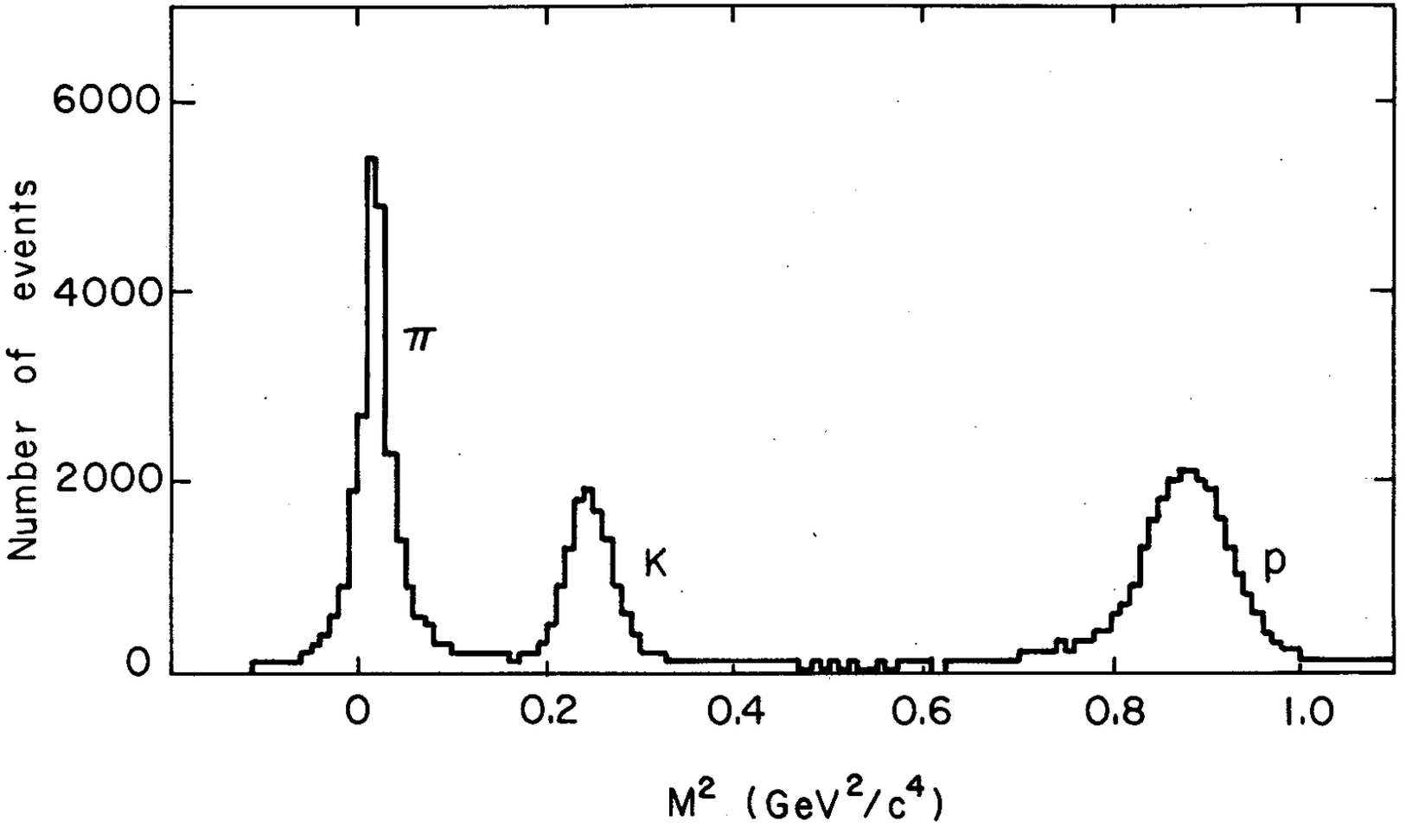

Fig. 15

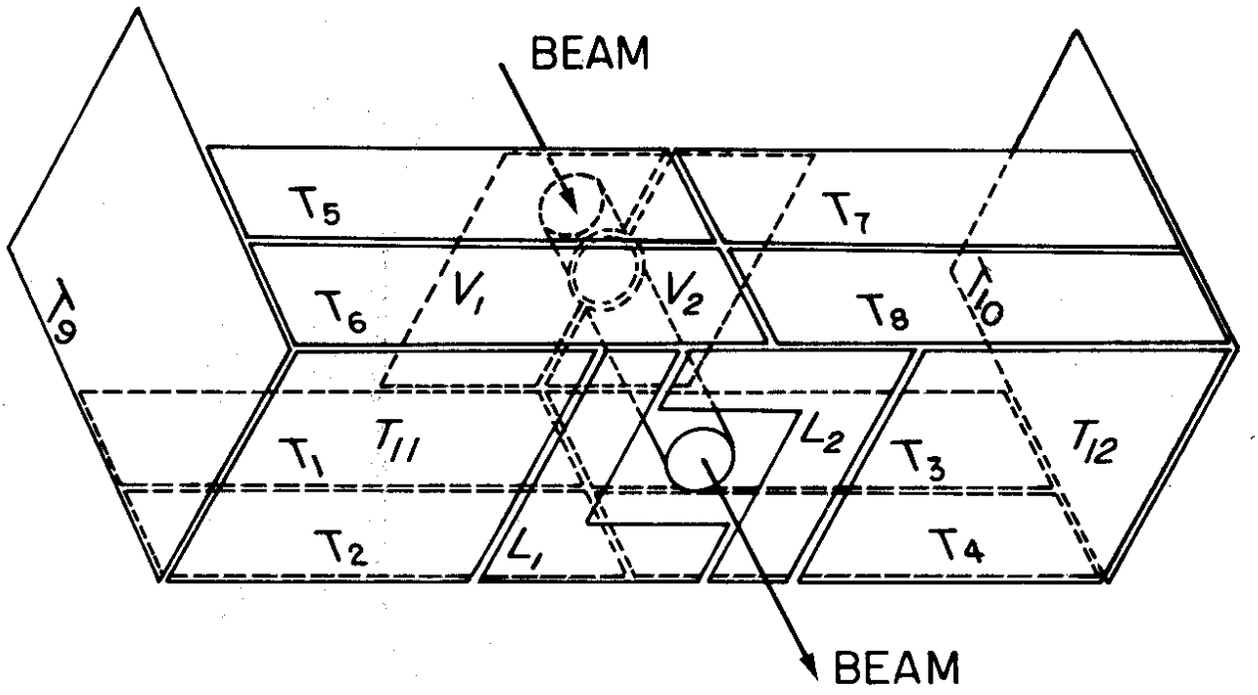

Fig. 16